Journal of Plankton Research Vol.19 no.11 pp.1713–1742, 1997

Estimation of the photosynthesis/irradiance (*P/I*) curve parameters from light and dark bottle experiments

R.H.Aalderink and R.Jovin

Department of Water Quality Management and Aquatic Ecology, Wageningen Agricultural University, PO Box 8080, 6700 DD Wageningen, The Netherlands

Abstract. Light and dark bottle experiments, carried out in three systems in the Netherlands, were used to estimate the parameters of models relating the oxygen production rate to incident light intensity. The maximum production rate (P_M) and the light saturation constant (I_S) were estimated using both gross and nett oxygen production data. In the latter case, the community oxygen consumption rate (R_{ox}) was also estimated. Eight models were compared with respect to goodness of fit, as has been accomplished previously by Jassby and Platt (*Limnol. Oceanogr.*, **21**, 540–547, 1976) and many others. This study, however, emphasizes the problem of parameter correlation and the consequential usefulness of these type of experiments to identify the *P/I* curve parameters. The results show that at a 90% level of confidence, the models cannot be distinguished with respect to goodness of fit. However, the models do show distinct differences in parameter correlation. Parameter correlation was shown to be related to the shape of the curve. *P/I* curves with high convexity were shown to be less sensitive for parameter correlation. In particular, models showing low convexity suffer from overparameterization, which means that on the basis of the observed production rates it is difficult to discriminate between the parameters. Also, alternative model formulations, using P_M and the initial slope (α), were investigated. These formulations produced less parameter correlation. However, for models with low convexity, showing high parameter correlation anyway, the reduction is limited. The use of nett oxygen production data does not show a significant difference in fit at a 90% confidence level. However, measured R_{ox} from dark bottle experiments tends to be higher than the values found by estimating R_{ox} from nett oxygen production.

Introduction

Light and dark bottle experiments have been applied for a long time (Talling, 1984). Typically, these experiments, in which the oxygen production or carbon assimilation rate is measured in bottles incubated at different depth in the water column, have been used to: calculate depth-integrated production (Vollenweider, 1974); determine spatial and temporal variation of assimilation numbers (Falkowski, 1981); investigate the variation of the physiological status of algal populations with changing environmental conditions or with imposed treatment (Côté and Platt, 1984); estimate the characteristic parameters for algal growth modelling (van Straten and Herodek, 1982). The methodological problems related to these experiments have been discussed at length by many authors. Harris (1984) shows that the effects of cell death, sinking and grazing during incubation may influence production estimates considerably, and Carpenter and Lively (1980) discuss the different light climate in the bottles compared to the water column, depending on the material of the bottles. They also show that the measured production depends greatly on the size of the bottles and relate this to the surface-to-volume ratio of the flasks used. Furthermore, as the bottles are incubated at a fixed depth, and whereas the phytoplankton in the free water column experience a wide range of light intensities due to vertical mixing, the

light climate is not representative both with respect to intensity and quality. This may result in the artificial inhibition very often observed in the bottles just below the water surface.

Besides the traditional light and dark bottles, more advanced incubators have been developed both for *in situ* and laboratory use. For example, Sakamoto *et al.* (1984) and van Duin *et al.* (1995) used long perspex tubes, and Tank and Musson (1993) developed a fully automated chamber, including data storage for measurements in the field. However, these devices partly suffer from the same experimental drawbacks.

Whatever method is used, the data produced all consist of photosynthetic rates observed at a number of increasing light intensities, and mostly are evaluated by estimating the parameters of a model describing the photosynthesis/irradiance (*P/I*) curve. A lot of work has been done in the past on the estimation of *P/I* curve parameters, and many authors tried to find the best model to describe the observed data (Jassby and Platt, 1976; Lederman and Tett, 1981; Field and Effler, 1982; Nicklisch, 1992). Also in this study, a number of models were compared with respect to goodness of fit and resulting parameter uncertainty. Oxygen production data from light and dark bottle experiments carried out in three systems in the Netherlands were used to carry out the analysis. However, as it is well known that the typical hyperbolic *P/I* curves easily suffer from overparameterization (Richter and Söndgerath, 1990), special attention was paid to the correlation between the parameters. Overparameterization means that, given the data, it is not possible to discriminate between the model parameters and, consequently, they are not adequately identified. In particular, if the parameters are used to assess the physiological status of the algae, highly correlated parameters are worthless. Overparameterization results both from the model structure and from the experimental design. For light and dark bottle experiments in shallow turbid systems in particular, the design is likely to be poor, as both the number of data points is limited and the distribution of the data over the *P/I* curve is far from optimal. As the experimental design cannot be controlled as well, the main goal of this study was to investigate the suitability of light and dark bottle experiments to estimate *P/I* curve parameters. Furthermore, we tried to identify the most appropriate model to estimate the parameters and to find the most suitable parameters to estimate.

Data description

Traditional light and dark bottle experiments (Vollenweider, 1974) were carried out in three systems in the Netherlands (Lake Wolderwijd, Lake Ankeveen and River Amstel). The basic characteristics of the system are presented in Table I.

The Lake Wolderwijd experiments have been described by van Duin *et al.* (1989). Lake Wolderwijd is a shallow lake, created in 1967 during the reclamation of the Polder Flevoland from the IJsselmeer basin. At the time of the experiments, the lake was highly eutrophic and dominated by the cyanobacterium *Oscillatoria agardhii*. Experiments were carried out in the summer of 1981 and 1982. The biomass, expressed as chlorophyll (Chl) *a*, ranged from 90 up to 250

Table I. Basic characteristics of the three systems where the experiments were carried out

System	Period	Mean depth (m)	Light attenuation coefficient (m^{-1})	Chlorophyll *a* ($\mu g\ l^{-1}$)	Dissolved inorganic P ($\mu g\ P\ l^{-1}$)	Dissolved inorganic N ($mg\ N\ l^{-1}$)
Lake Wolderwijd	Summer 1981 Summer 1982	1.6	4–10	90–250	2–75	No data available
Lake Ankeveen	Summer 1991 Autumn 1991	1.2	1–5	15–45	20	0.07–0.50
River Amstel	Spring 1989 Autumn 1989	3.2	3–8	60–250 10–50	100–200	5.0–9.0

$\mu g\ l^{-1}$. Light attenuation coefficients were high. Suspended solids contribute significantly to the total extinction as wind-induced resuspension is high due to the long fetch at the prevailing wind direction in this shallow lake. As dissolved inorganic phosphorus (P) was very low during some experiments (see Table I), P limitation may have occurred in some of the experiments. Dissolved inorganic nitrogen was not measured, but nitrogen is not considered to be growth limiting (van Duin and Lÿklema, 1989).

Lake Ankeveen is a shallow mesotrophic lake in the centre of the Netherlands. During the last 10 years, the external P loading of the lake has been reduced and additional measures have been taken to restore the lake ecosystem (Roijackers and Verstraelen, 1988). In Lake Ankeveen, the experiments were carried out during late summer and autumn of 1991. Through the sampling period, the system was dominated by Chlorophyta (*Chlorococcalis*) and Bacillariophyta (*Stephanodiscus*, *Diatonema*, *Surirella*). At the end of the summer, a small bloom of Cyanophyta (*Hormogonales*) was observed. The system can be characterized as moderately productive and moderately eutrophic. Dissolved inorganic P did not vary much. The average concentration was ~20 $\mu g\ P\ l^{-1}$. Both the ammonia and nitrate concentrations did show an increase towards the end of the measuring period.

The Amstel is a river south of Amsterdam. It is mainly fed by superfluous water from the adjacent polders. The average residence time in some parts of the river is high (up to 50 days) and algal blooms do occur frequently (Aalderink *et al.*, 1994). Data were collected in the spring and autumn of 1989. Nutrient levels were high. During spring, the system was dominated by diatoms, predominantly *Melosira varians*. Biomass varied from 60 to 250 μg Chl *a* l^{-1}. During the autumn of 1989, biomass was low, varying between 10 and 50 μg Chl *a* l^{-1}. For this period, no specific information on the algal species was available.

During the Amstel and Ankeveen experiments, light was measured continuously at two depths. Five minute averaged readings were stored in a data logger. From the intensities measured at both depths, the light attenuation coefficient and the light intensity at the water surface were calculated. This procedure assumes a constant light attenuation coefficient over depth. As the spectral distribution of the irradiance changes with depth towards the most penetrating wavelengths, in many systems a decrease in the vertical attenuation coefficient is found. However, in shallow turbid systems this effect is not very distinct as, due

to scattering, the path length of the photons increases with depth, leading to higher values of the attenuation coefficient at greater depth (Kirk, 1977).

The 5 min values served as the input for the model used to estimate the parameters. For the Wolderwijd experiments, only averaged light intensities and attenuation coefficients over the exposure time were available. The light and dark bottle experiments were carried out in duplicate or triplicate, incubating samples at five or six depths. Incubation times varied between 1 and 4 h, depending on the biomass present.

Mathematical description

In the literature, many equations can be found that describe the relationship between the observed carbon assimilation (or oxygen production rate) and incident light intensity. Most of these equations are empirical, although some do have a physiological background to a certain extent (Fasham and Platt, 1983; Megard *et al.*, 1984; Eilers and Peeters, 1988). Also, dynamic models, incorporating the effect of light history on light efficiency, inhibition and the time lag in the response to changing light conditions, have been developed (Lewis *et al.*, 1984; Denman and Marra, 1986; Pahl-Wostl and Imboden, 1990; Eilers and Peeters, 1993). A

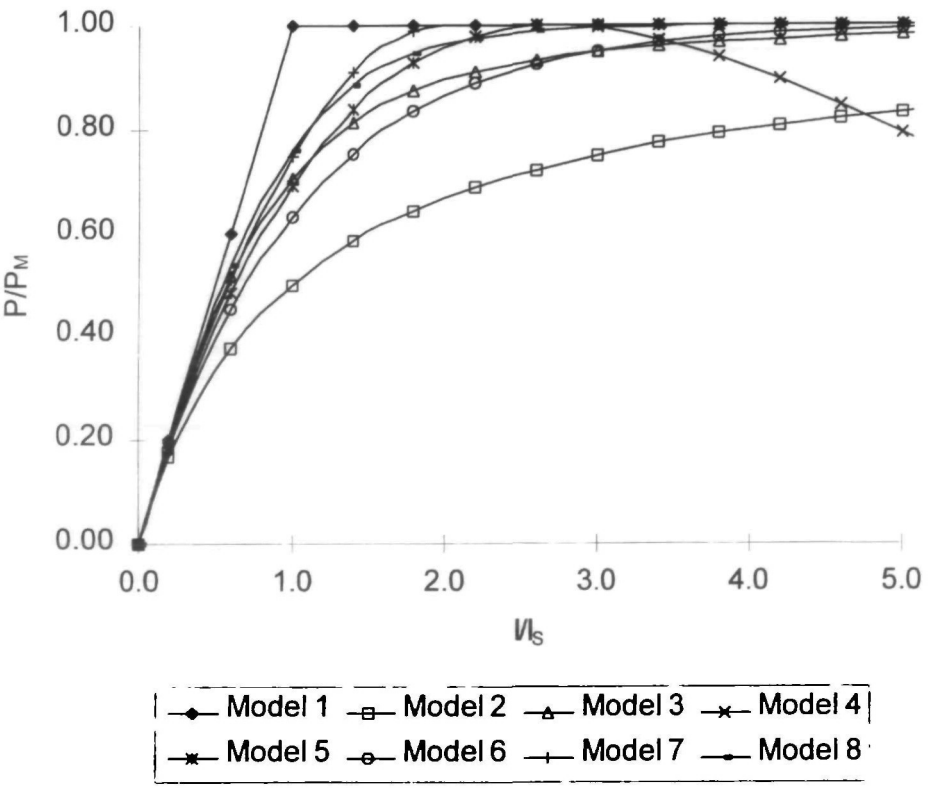

Fig. 1. *P/I* curves according to the eight different models presented in Table I.

discussion of these mechanistic and dynamic models is not within the scope of this paper. The empirical models discussed here all try to describe the three well-known phenomena found in the response of photosynthesis to increasing light intensity (see Figure 1). At low intensities, production is proportional to light intensity. With increasing light, the slope is decreasing until complete light saturation. At saturating intensity, the slope equals zero and the maximum photosynthetic rate is reached. Within the photoinhibited range, the rate of change becomes negative and production decreases with increasing light intensity.

Figure 1 shows the *P/I* relationship according to eight different models found in the literature. These are the equations, as they have been compared by Jassby and Platt (1976) and later by others (Lederman and Tett, 1981; Field and Effler, 1982; Nicklisch, 1992). An overview of the equations is given in Table II. Except for the Steele model, all equations describe the *P/I* relationship within the non-inhibited range. These typical hyperbolic equations can be characterized by two parameters, P_M and α, representing the maximum production rate and the initial slope at low light intensity. Another way to formulate the models, proposed by Talling (1957), is to introduce the parameter I_S. I_S, the light saturation constant, equals the light intensity at the intersection of the maximum production rate and the line found by extrapolation of the initial slope of the curve. The advantage of the use of I_S is that it is independent of biomass and, therefore, I_S is frequently used as a characteristic parameter for comparison of the photoacclimation status of the algae (Henley, 1993). The model formulation using I_S is also usually applied in eutrophication modelling. In the US Environmental Protection Agency models

Table II. Two-parameter empirical *P/I* models. P_M is the maximum oxygen production rate (g O_2 m^{-3} h^{-1}), I_S is the light saturation constant (W m^{-2}) and I_{opt} (in models 4 and 5) is the optimal light intensity (W m^{-2})

Model 1	$P(I) = P_M \frac{I}{I_s}$ $I \le I_s$ $P(I) = P_M$ $I > I_s$	Blackman (1905)
Model 2	$P(I) = P_M \frac{I/I_s}{1 + I/I_s}$	Baly (1935)
Model 3	$P(I) = P_M \frac{I/I_s}{\sqrt{1 + (I/I_s)^2}}$	Smith (1936), Talling (1957)
Model 4	$P(I) = P_M \frac{I}{I_{opt}} \exp\left(1 - \frac{I}{I_{opt}}\right)$	Steele (1962)
Model 5	$P(I) = P_M \frac{I}{I_{opt}} \exp\left(1 - \frac{I}{I_{opt}}\right)$ $I \le I_{opt}$ $P(I) = P_M$ $I > I_{opt}$	Jassby and Platt (1976)
Model 6	$P(I) = P_M [1 - \exp(-I/I_s)]$	Web *et al.* (1974)
Model 7	$P(I) = P_M[\frac{I}{I_s} - 0.25 (\frac{I}{I_s})^2]$ $I \le 2I_s$ $P(I) = P_M$ $I > 2I_s$	Jassby and Platt (1976)
Model 8	$P(I) = P_M \tanh(\frac{I}{I_s})$	Jassby and Platt (1976)

like QUAL2E and EUTROWASP, typically depth-averaged *P/I* curves are used to describe primary production, using I_S (or I_{opt} for the Steele model) to control the shape of the curve.

As the experimental method implies the measurement of the change in the oxygen concentration in the light and dark bottles, the equations presented in Table II must be incorporated in a model describing the production and consumption of oxygen in the bottles fixed at a particular depth. Equation (1) describes the change in the oxygen content at depth z:

$$\frac{dO_2}{dt}\Big|_z = P_M F_{L,z} - R_{ox} \tag{1}$$

where $F_{L,z}$ is the light limitation factor (–) as given by models 1–8 (Table II) and R_{ox} is total community oxygen consumption (g O_2 m^{-3} h^{-1}).

If ample nutrients are available, P_M equals the non-nutrient-limited maximum production rate. If nutrient limitation occurs, P_M should be considered as a nutrient-limited rate (van Straten and Herodek, 1982). R_{ox} also includes, besides the algal respiration, the oxygen consumption due to the biochemical oxidation of detritus and non-algal organic matter. Assuming R_{ox} to be constant during the experiment, the nett oxygen production in a bottle at depth z can be calculated from:

$$NOP_z = P_M \int_0^\tau (F_{L,z})dt - R_{ox}\tau \tag{2}$$

where NOP_z is the nett oxygen production (g O_2 m^{-3}) and τ is the exposure time (h).

In the same way, the gross production GOP_z can be evaluated using:

$$GOP_z = \int_0^\tau \left(\frac{dO_2}{dt}\Big|_z + R_{ox}\right) dt = P_M \int_0^\tau F_{L,z} \tag{3}$$

Both equations (2) and (3) can be evaluated numerically using a discrete time interval Δt:

$$NOP_z = P_M \sum_{i=1}^{n} (F_{L,z,i})\Delta t - R_{ox}\tau \tag{4}$$

$$GOP_z = P_M \sum_{i=1}^{n} (F_{L,z,i})\Delta t \tag{5}$$

The time step Δt equals the time interval between the light measurements. The number of time intervals n equals $\tau/\Delta t$. Average nett and gross production rates can be obtained by dividing *NOP* and *GOP* by the exposure time τ. The use of equations (4) and (5) makes it possible to use detailed recorded light intensities

if available. However, often only averaged values of light intensities are available. For example, during the experiments in Lake Wolderwijd, light was measured using a cumulative photoquantum sensor, resulting in exposure time-averaged values for the light intensity. In that case, the model equations should be reformulated and $F_{L,z}$ should be calculated using average light intensities. However, on days showing varying cloud cover, the light intensity during the experiment can be highly variable and the use of averaged values might influence the results.

Parameter estimation

Many efforts have been made to estimate the parameters in the *P/I* relationship and several methods have been applied. Before the introduction of computers on a wide scale, several authors tried to estimate the parameters by transformation of the non-linear equations in a linear form. For example, the Monod type of equation according to model 2 can be rewritten in such a way that linear regression of $1/P$ upon $1/I$ results in an estimate of P_M from the intercept and of I_S from the regression slope. Also, the Smith relationship (model 3) can be transformed in such a way that linear regression can be applied (Talling, 1957). However, linear transformation of these hyperbolic type of equations very often results in biased estimates of the parameters (Lederman and Tett, 1981). The use of non-linear parameter estimation methods, based on the minimization of the sum of squared errors, is less sensitive to these problems. An early example of the use of non-linear parameter estimation methods applied to *P/I* curves is given by Jassby and Platt (1976). They initially applied the well-known Marquard algorithm to estimate α ($1/I_S$) and P_M, but reported that the method led to spurious results and concluded that the simultaneous estimation of the parameters was not possible. Consequently, they estimated the parameters using a sequential method. They first estimated R_{ox} and α using linear regression on the linear low-light part of the *P/I* curve. Subsequently, they used a direct grid search method to estimate P_M. Lederman and Tett (1981) showed that the sequential method applied by Jassby and Platt also results in biased estimates of the parameters and showed that the use of non-linear parameter estimation methods was possible. They used Bard's (1974) methods using a maximum likelihood criterion. Later on, numerous applications of simultaneous non-linear methods could be found in the literature. Platt and Gallegos (1980a) and Gallegos and Platt (1981) used a modified Gauss–Newton method. The Marquard algorithm has been applied successfully by Field and Effler (1982, 1984), Neale and Marra (1985) and Zimmerman *et al.* (1987). Peterson *et al.* (1987) used an exponential least square method.

An efficient method has been presented by van Straten and Herodek (1982). Their method is based on simultaneous linear and non-linear regression. As the model equations [equations (4) and (5)] are linear in P_M and R_{ox}, these parameters can be estimated directly through solving the linear normal equations. The normal equations can be found by setting the derivatives with respect to the parameters of the least square sum expression equal to zero. For the description of the nett oxygen production [equation (4)], the expression for the sum of squared residuals is given by:

$$SSE(P_M, I_S, R_{ox}) = \sum_{j=1}^{m} (NOP_{Obs,j} - NOP_j)^2 \quad (6)$$

in which $SSE(P_M, I_S, R_{ox})$ is the sum of the squared residuals between the model and measurements, $NOP_{Obs,j}$ is the observed nett oxygen production during the exposure time at depth z (g O^2 m^{-3}) and m is the number of light bottle measurements (–).

The two resulting linear normal equations are given by:

$$P_M \sum_{j=1}^{m} (A_j)^2 - R_{ox}\tau \sum_{j=1}^{m} (A_j) = \sum_{j=1}^{m} (NOP_{Obs,j}\, A_j) \quad (7)$$

$$-\tau\, P_M \sum_{j=1}^{m} (A_j) + m\tau^2\, R_{ox} = -\tau \sum_{j=1}^{m} (NOP_{Obs,j}) \quad (8)$$

in which:

$$A_j = \sum_{i=1}^{n} F_{L,j,i}\, \Delta t \quad (9)$$

Differentiating equation (6) with respect to I_S, and setting the result equal to zero, leads to the following non-linear equation:

$$P^2{}_M \sum_{j=1}^{m} \left(A_j \frac{\partial A_j}{\partial I_S}\right) - R_{ox}\tau\, P_M \sum_{j=1}^{m} \left(\frac{\partial A_j}{\partial I_S}\right) = P_M \sum_{i=1}^{m} \left(NOP_{Obs,j} \frac{\partial A_j}{\partial I_S}\right) \quad (10)$$

Van Straten and Herodek (1982) solved this equation using a zero-finding routine. We did not solve equation (10), but used a direct optimization method to minimize the sum of squares as a function of I_S. The overall procedure is illustrated in Figure 2. Starting from an initial estimate of I_S, the linear normal equations are solved for R_{ox} and P_M, and subsequently the sum of squared residuals is evaluated. This procedure is repeated until a pre-defined stopping criterion is met. The golden section method (Press *et al.*, 1989) was used to minimize *SSE* with respect to I_S. In this way, the three-dimensional optimization problem has been reduced to a one-dimensional one, resulting in an efficient estimation algorithm. The parameters of the two-parameter model according to equation (5) can be estimated in the same way. In that case, there is only one linear normal equation to be solved.

As the model is non-linear in I_S, only an approximation of the covariance matrix of the parameters can be given (Draper and Smith, 1981):

$$COV(\hat{P}_M, \hat{R}_{ox}, \hat{I}_S) = (\hat{B}^T \hat{B})^{-1} \hat{s}^2 \quad (11)$$

in which B is the Jacobian matrix, for which the elements are given by the derivatives of the model equation with respect to the parameters. B^T is the transposed matrix of B and and $\hat{s}^2$ is an estimate of the residual error variance:

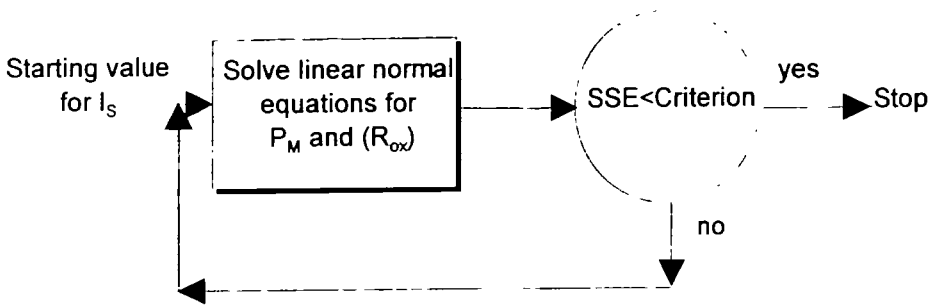

Fig. 2. Parameter estimation procedure.

$$s^2 = SSE(\hat{P}_M, \hat{R}_{ox}, \hat{I}_S)/(m-p) \tag{12}$$

The standard deviation and the confidence intervals for the individual parameters can be calculated from the diagonal elements of the covariance matrix. A $(1-\beta)$ confidence interval for the ith parameter can be defined as:

$$\theta_i \pm t\,(m-p, 1-\beta/2)\sqrt{COV(i,i)} \tag{13}$$

in which θ_i is the ith parameter and $t(m-p, 1-\beta)$ is the $1-\beta/2$ quantile of the t distribution with $m-p$ degrees of freedom.

An approximate joint $(1-\beta)$ confidence region for all parameters is given by:

$$SSE(\theta) = SSE(\hat{\theta})\left[1 + \frac{p}{m-p} F(p, m-p, 1-\beta)\right] \tag{14}$$

in which $F(p, m-p, 1-\beta)$ is the $1-\beta$ upper point of the $F(p, m-p)$ distribution.

Equation (14) represents the contour that encloses the $(1-\beta)$ confidence region. Although the contour is exact, the confidence level is not, as the model is not linear in all parameters (Draper and Smith, 1981). In the linear case, these contours are elliptically shaped. For models non-linear with respect to the parameters, this is generally not the case. The contour can be calculated in a straightforward way, as shown by van Straten and Herodek (1982). By varying I_S, the two roots of the quadratic equation (14) can be calculated directly. From the confidence intervals for the individual parameters, a confidence region can also be constructed, but in particular if the parameters are correlated, the joint confidence regions can be much wider. A measure for the parameter correlation can be obtained from the covariance matrix as well. The linearized approximate correlation between the ith and jth parameters is given by:

$$\rho_{i,j} = \frac{COV(i,j)}{\sqrt{COV(i,i)\cdot COV(j,j)}} \tag{15}$$

A high correlation between the parameters indicates that the model is overparameterized, which means that given the data it is not possible to discriminate between the correlating parameters or that the model itself is degenerated with respect to these parameters. In the latter case, the model should be reformulated, and in the first case the experiments should be redesigned (Richter and Söndgerath, 1990). High parameter correlation leads to non-unique parameter estimates, as a wide range of parameter combinations result in approximately the same sum of squared residuals. This is also illustrated by the shape of the joint confidence region. For high parameter correlation, the contours are very often quite elongated and oriented with respect to the parameter axes.

Results

Figure 3 shows the estimated and measured oxygen production rates for one of the experiments from the Amstel data set. The estimated parameters and least square sums for all eight models are presented in Table III. As the input for the model, the mean light intensity over the exposure time was used. The average light intensity equalled 132 W m^{-2}, the extinction coefficient was 5.3 m^{-1} and Chl *a* concentration was 57 $\mu g\ l^{-3}$. Both I_S and P_M in the two-parameter model for gross oxygen production have been estimated. The results are typical for the analysis of the data from all the other experiments. Although the least square sum does show some differences, all models describe the data reasonably well. Model 2 results in the highest least square sum and model 4 shows the lowest. For all models, the coefficient of variation for I_S, calculated as the quotient of the standard deviation and the value of the parameters at the best fit, is higher than for P_M. Model 2 shows the highest coefficient of variation for both parameters. Model 2 also shows a rather high correlation between P_M and I_S, indicating overparameterization, as also demonstrated by the 90% confidence contour plot presented in Figure 4. In Figure 4, both the joint 90% confidence region and the 90% confidence intervals for the separate parameters have been plotted. As can be seen for model 4, showing the lowest correlation coefficient between the parameters, the 90% confidence region is narrow and there is good agreement with the 90% individual parameter interval. For model 2, having a correlation coefficient between I_S and P_M of 0.89, the 90% confidence contour is far more elongated and

Table III. Estimated parameters for experiment AMS21 from gross oxygen production for all eight models

Model	P_M ($g\ O_2\ m^{-3}\ h^{-1}$)	CV (%)	I_S ($W\ m^{-2}$)	CV (%)	*r*	*SSE*
1	0.815	2.7	25.2	6.0	0.45	0.0029
2	1.098	11.2	19.1	29.9	0.89	0.0126
3	0.890	4.0	22.3	10.3	0.75	0.0034
4	0.877	0.8	57.1	1.7	0.31	0.0003
5	0.839	1.7	52.9	4.4	0.70	0.0007
6	0.869	4.6	18.0	12.2	0.76	0.0045
7	0.826	1.4	21.2	3.3	0.68	0.0005
8	0.845	2.2	22.4	5.7	0.68	0.0014

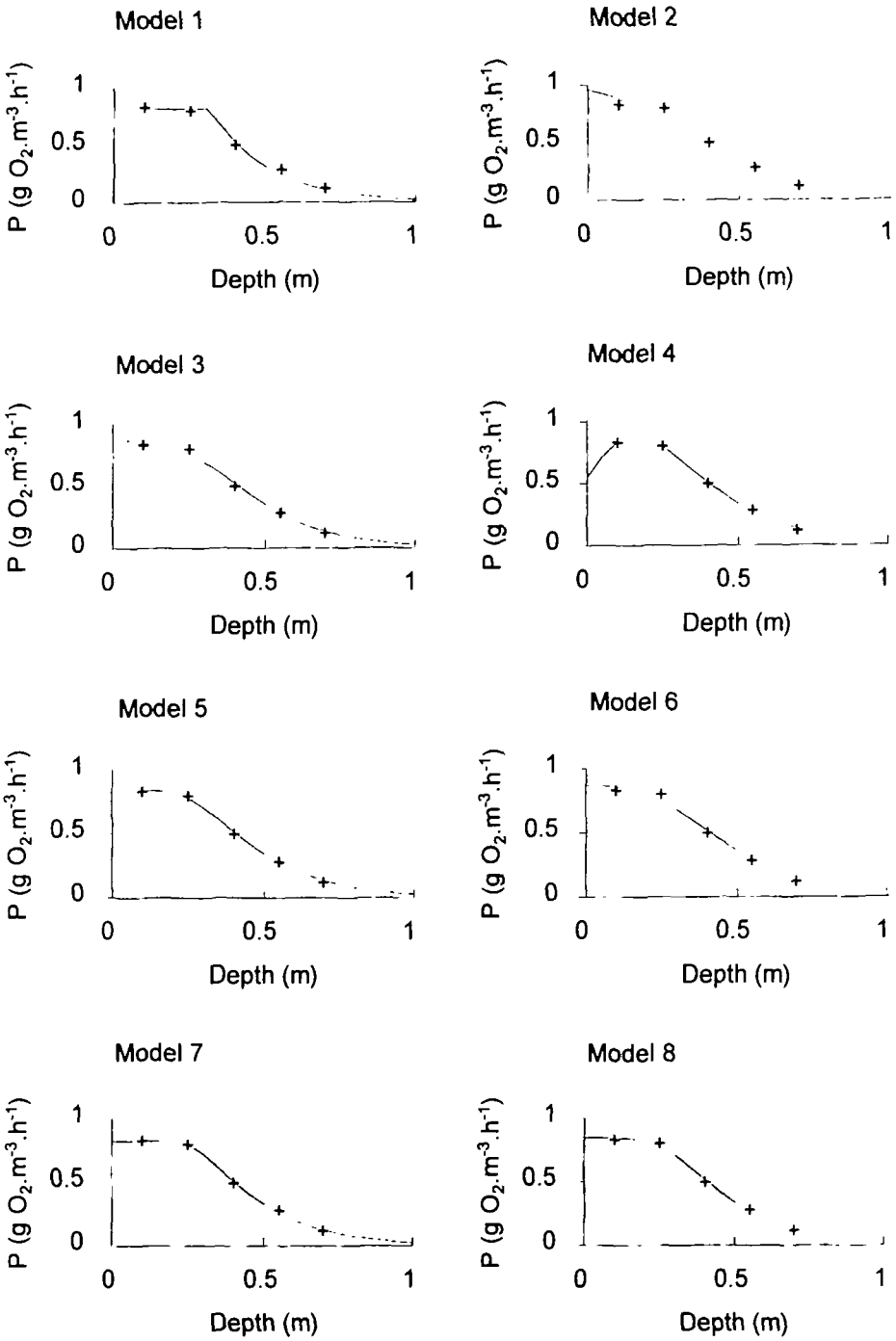

Fig. 3. Simulated and observed oxygen production rate for experiment AMS21.

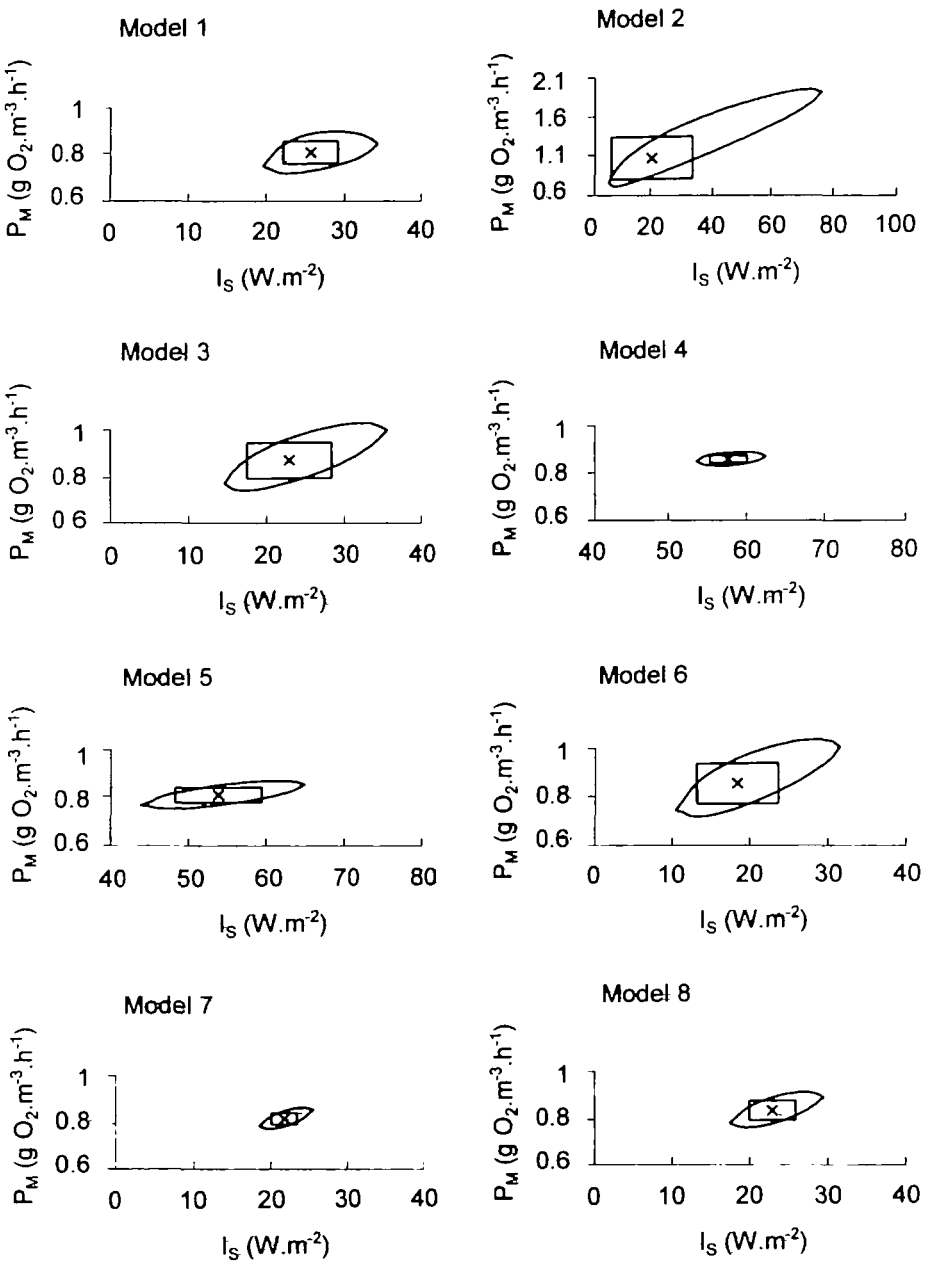

Fig. 4. Joint confidence regions for the parameters estimated from experiment AMS21 data.

a strong dependency between the parameters is apparent. The estimated values of P_M for all models, except for model 2, fall within a close range and also there is no profound variation between the estimated values for I_S. By definition, for model 4 and 5 I_{opt} is a factor 2.71 greater than I_S.

Goodness of fit

Table IV presents the resulting grand sum of squared residuals for the eight models applied to the gross oxygen production data from Lake Wolderwijd. In total, 27 experiments were carried out measuring the oxygen produced at five or six depths. Model 5 showed the lowest sum of squared residuals. For each model, an *F*-test statistic was calculated by dividing the resulting sum of squares by the one found for model 5. The grand number of degrees of freedom equals 90, which was found by adding the degrees of freedom of the individual experiments. The critical value for the *F*-test at a 90 or 95% confidence level and at 90/90 degrees of freedom equals 1.417 or 1.321, respectively, which means that none of the models significantly fits worse than model 5. The square root of the mean square error SSE_{tot}/total degrees of freedom (Richter and Söndgerath, 1990) varies from 0.17 to 0.19 mg O_2 l^{-1}, which is comparable to the measurement error within the experimental data. An estimate of the measurement error in the data has been obtained from a number of triplicate experiments within the Amstel data set and resulted in ~0.2 mg O_2 l^{-1}. This means that it is likely that an important part of the sum of residual squares is explained by the measurement error and none of the models shows a significant lack of fit.

A number of other authors did compare the goodness of fit for different *P/I* relationships. Jassby and Platt (1976) were probably the first who compared a number of models to real data to find the best relationship to describe *P/I* data. They estimated both the initial slope α and P_M using data from light-saturating measurement from stations in the coastal waters of Nova Scotia. Using their sequential method, they estimated the parameters from the eight models presented in Table II and examined the results on the basis of the residual sum of squares. For each station, they calculated the mean squared deviation over all experiments as a measure of goodness of fit for all models. Furthermore, for each model they determined the number of experiments for which the fit was best (N_i). For all three stations, they found that the model according to Smith (model 3) resulted in the best overall fit, directly followed by model 8. Model 4 (Steele) showed by far the highest mean square deviation for each station. On the basis of ranks of N_i, they concluded however that model 8 (hyperbolic tangent) was the best model, as this model fitted the data best for 38% of all experiments. Model 3

Table IV. Comparison of overall goodness of fit for the eight models applied to Lake Wolderwijd data

Model	SSE_{tot}	*F*	CV P_M	CV I_s/ CV I_{opt} (model 4, 5)	ρ
1	3.022	1.12	8.5	24.5	0.40
2	2.913	1.08	16.8	60.7	0.82
3	2.879	1.07	11.2	41.7	0.66
4	3.386	1.26	10.5	20.9	0.35
5	2.691	1.00	10.0	33.7	0.56
6	2.717	1.01	11.6	41.1	0.65
7	2.729	1.01	9.2	30.1	0.53
8	2.838	1.05	10.0	35.3	0.59

was the second best in 28% of the experiments. Lederman and Tett (1981) commented on the use of N_i as it is a statistic of undefined properties. Hence, on the basis of N_i, it is not possible to prove a statistically significant difference between the models. They found a poor correlation between the overall mean squared deviation and the rank based on N_i. This could be expected, as N_i does not take the absolute differences of the goodness of fit between the models into account as the overall deviation does. So the latter can be highly influenced, for example, by a small number of high least square sum values, whereas N_i is not. On the basis of the original results of Jassby and Platt, Lederman and Tett showed, using an F-test, that models 8 and 3 indeed fitted significantly better than the others, although no distinction between the two could be made. Estimating the parameters again from the same data sets, using a simultaneous method instead of the sequential method, showed that models 1, 2 and 4 fitted significantly worse and that no distinction could be made between the other models. It is striking that the grand least square sums found by Lederman and Tett were more than a factor of 10 smaller than the values found by Jassby and Platt.

Another example in which a number of models was compared is given by Field and Effler (1982). Using data from Onondaga Lake, they estimated the parameters of models 2–7 and compared the resulting sum of squares. They grouped the data from all productivity experiments (115) together and used these as one data set (n = 522) and applied the Marquard algorithm to estimate the parameters. On the basis of the resulting least square sum, they concluded that models 4 and 7 are not suitable to describe their data. However, calculating an F-statistic for the reported least square sums shows that only model 7 fits significantly worse than the others. The use of grouped data from several experiments, probably distributed over a longer time period (temperature ranged from 7 to 26°C), is probably not the most suitable set-up for comparing the fit of several models. It can be assumed that much of the overall sum of squared residuals is explained by the variability in the specific production between the experiments and by the unrealistic assumption of constant parameters over the total period in which the experiments took place. Within their analysis, however, they corrected for temperature, as they included temperature dependency in their models. However, temperature is only one of the explanatory factors for the variability in the model parameters.

Nicklisch (1992) also compared a number of relationships on the basis of the sum of squared residual errors. He used laboratory data from a culture of the blue–green alga *Limnothrix redekei* relating growth rate to continuous illumination in the range of 0–10 mol m^{-2} day^{-1}. He concluded that models 2 and 6 fitted the data best. The exponential model (model 6) resulted in the lowest sum of squares, but the difference between both models was not significant at a 95% confidence level.

As the use of the grand sum of squared residuals could be influenced by a few experiments showing large *SSE* values, the goodness of fit for the individual experiments was also examined. Figure 5 shows the F ratios for the 27 individual experiments in Lake Wolderwijd. For each data set and model, the ratio of the sum of squared residuals and the minimum residual sum was calculated. In

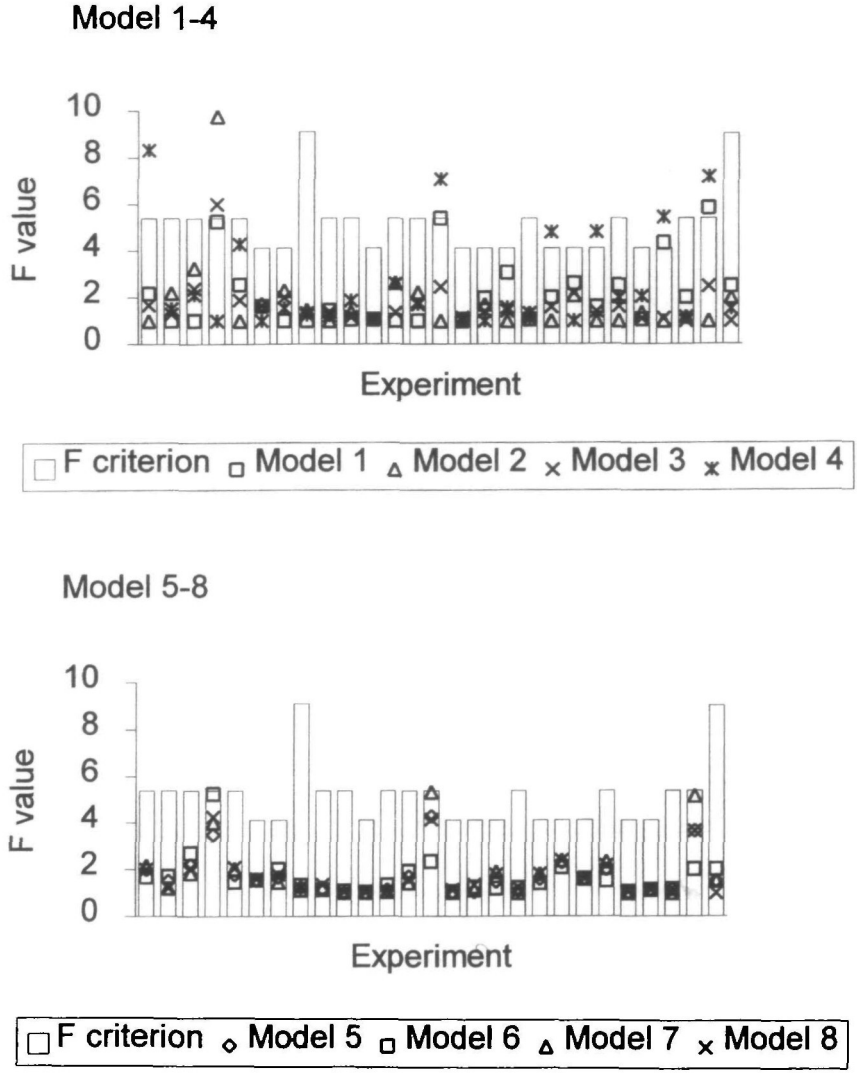

Fig. 5. Comparison of the goodness of fit for the individual experiments from the Wolderwijd data set.

Figure 5, the critical F value for each experiment is also indicated. This value is not the same for all experiments, as the number of observations differs. For the sake of clarity, Figure 5 is split into two parts. Models 1–4 are presented in the upper figure and the lower side figure presents models 5–8.

Models 5–8 do not fit significantly worse than the model resulting in the lowest sum of squares. For six out of the 27 experiments, model 4 (Steele) shows a significantly poorer fit than the best model. For model 1, two experiments result in a poorer fit, and models 2 and 3 show a significantly inadequate fit for only one experiment. Eliminating the six experiments for which model 4 did fit significantly

worse resulted in a grand sum of squares for all models which was in the same range. Hence, the use of the grand sum can be somewhat misleading. A detailed analysis showed that the six experiments, for which model 4 did not describe the data significantly well, clearly showed saturation at high light intensity. That means that in the two topmost bottles the oxygen production was almost the same. In that case, the use of model 4, which includes inhibition, produces a poor fit. In case the data do not show this plateau in production, model 4 is perfectly able to describe the data, as is shown in Figure 3.

Coefficients of variation

Although the coefficients of variation of the individual parameters differ significantly from experiment to experiment, the average values presented in Table IV do give a good impression of the dissimilarity between the eight model equations. For all models, the coefficient of variation of P_M was smaller than that for I_S. The order of magnitude is in agreement with the results found by Zimmerman *et al.* (1987) for model 6, using *P/I* curves with <10 data points. Van Straten and Herodek (1982) estimated the parameters for model 4 using ^{14}C uptake experiments conducted at four depths in Lake Balaton. The coefficients of variation found for both P_M and I_S were somewhat higher than those found for the oxygen production experiments in Lake Wolderwijd. Comparison of the results for the different models shows that, except for model 2, the coefficients of variation for P_M are similar (Table IV). Model 2 also results in the highest coefficient of variation for I_S, whereas the smallest value is found for model 4.

Zimmerman *et al.* (1987) compared the estimates for the coefficients of variation obtained by the linear approximation method according to equation (11) with the Monte Carlo approach. For the latter method, the parameters are estimated for a great number of noise-corrupted data sets and the statistics of the resulting parameter space are evaluated (Press *et al.*, 1989). They found that for poor-quality data and a limited number of observations, the linear approximation method tends to underestimate the coefficient of variation for the parameters. In particular, for the initial slope α and I_S, the discrepancy between both methods was prominent. However, direct comparison of the two methods is not possible, because calculation of the parameter variance from equation (11) does not take the correlation between the parameters into account, whereas the Monte Carlo approach does.

Parameter correlation

Table IV also presents the averaged correlation coefficients between the parameters of the model. Because it is once again also interesting to look at the parameter correlation for the individual experiments, Figure 6 shows the cumulative distribution of the correlation coefficients for the eight models. For model 4, the absolute value of the correlation coefficient is plotted as the correlation can be both negative or positive, depending on the ratio between I_{opt} and the ambient irradiance. For most of the experiments, model 4 displays the lowest correlation between the parameters. Only three data sets have a $\rho > 0.90$. For model 1, the

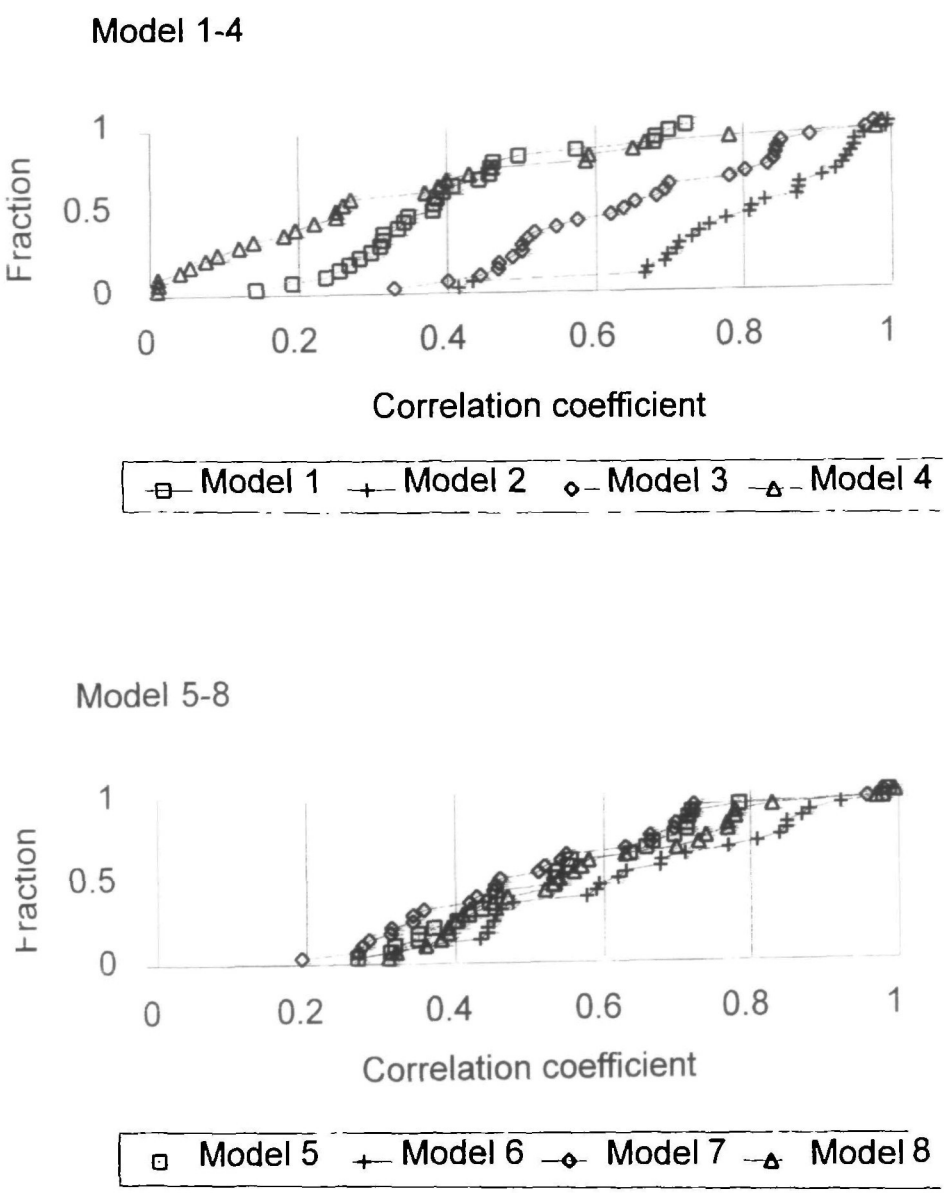

Fig. 6. Cumulative distribution of the correlation coefficient between I_S and P_M estimated from the Wolderwijd data set.

maximum correlation is 0.70. The highest correlations are found for model 2, having a mean value for ρ of 0.82 and ~60% of the experiments result in a correlation >0.80. Models 3 and 6 also show considerable correlation. For both models, the fraction having a correlation coefficient >0.80 is ~30%. For the other models, only a few experiments show high parameter correlations.

For the two-parameter model describing gross oxygen production [equation (5)] the expression for the correlation coefficient [equation (15)] can be expanded to:

$$\rho = \frac{\sum_{j=1}^{m} \left[\frac{\partial GOP_j}{\partial P_M} \cdot \frac{\partial GOP_j}{\partial I_S}\right]}{-\sqrt{\sum_{j=1}^{m} \left[\frac{\partial GOP_j}{\partial P_M}\right]^2} \cdot \sqrt{\sum_{j=1}^{m} \left[\frac{\partial GOP_j}{\partial I_S}\right]^2}} \qquad (16)$$

In general, for linear models, ρ is independent of the parameters and is completely determined by the independent variables. From equation (16), it follows that ρ is independent of P_M as the model is linear with respect to this parameter, and as the model is not linear in I_S, ρ is still a function of I_S. Furthermore, the correlation coefficient depends on the distribution of the light intensities over the *P/I* curve, which is controlled by I_0, the light attenuation coefficient and the depth the bottles have been fixed.

The differences in shape of the *P/I* curves are responsible for the differences in parameter correlation. The curves differ in convexity (curvature). A high convexity results in a long quasi-linear trajectory even at increasing light intensity. *P/I* curves with a low convexity (e.g. model 2) show a relatively fast decrease of the slope with increasing *I*. This indicates a gradual transition from light limitation to saturation. For the quadratic type of models, Leverenz *et al.* (1990) use $\theta_{0.5}$ as an index for the convexity of the curve. The convexity of the general non-rectangular hyperbola can be expressed on the basis of the model by Prioul and Chartier (1977):

$$\theta_{0.5} = 2\left(1 - \frac{I_{1/2}}{I_S}\right) \qquad (17)$$

where $I_{1/2}$ is the half-saturation light intensity.

Although only models 1 and 2 belong to the family of these quadratic hyperbola, Henley (1993) nevertheless used equation (17) to estimate convexity for a number of other models as well. Applying equation (17) for the models used in this study results in the $\theta_{0.5}$ values presented in Table V. In the lower part of the *P/I* curve, $\theta_{0.5}$ gives a reasonable estimate of the convexity; however, it underestimates the convexity of the non-quadratic models at higher light intensities. In particular for models 4, 5 and 6, showing a low $\theta_{0.5}$ compared to the other models, the convexity of the curve at light intensities above I_S is much higher as the slope in this region of the *P/I* curve is decreasing relatively slowly. For example, models 4 (5) and 3 intersect at approximately $I = I_S$ and at higher light intensities the model 4 curve clearly lies above the one for model 3, as can be seen from Figure 1. This is also illustrated by evaluating equation (17) at $I = 80\%$ of the saturating light intensity ($\theta_{0.8}$ in Table V), which is higher for models 4 and 5 than for model 3. In order to compare the overall convexity for all models, a modified shape

Table V. Convexity of the *P-I* model equations

Model	Convexity $\theta_{0.5}$	Convexity $\theta_{0.8}$
1	1.000	1.000
2	0.000	0.250
3	0.845	0.354
4	0.741	0.438
5	0.741	0.438
6	0.614	0.368
7	0.828	0.500
8	0.901	0.420

index θ^* has been defined, equal to the ratio between the slope of the *P/I* curve at $I = I_S$ and the initial slope (at $I = 0$):

$$\theta^* = \frac{\frac{\partial P(I)}{\partial I}\Big|_{I = I_S}}{\frac{\partial P(I)}{\partial I}\Big|_{I = 0}} \tag{18}$$

There is a distinct relationship between the parameters' correlation coefficient and the modified shape index. In Figure 7, the average correlation coefficients resulting from the Wolderwijd experiments are plotted against the shape index. It can be seen that for high-convex curves the correlation between the parameters is less. For these curves, it is likely that at relatively low I/I_S ratios one or more data points lie within the saturated range of the *P/I* curve. In that case, the correlation between the parameters is low and the model less overparameterized. For low-convexity models, however, this is not the case. For instance, for model

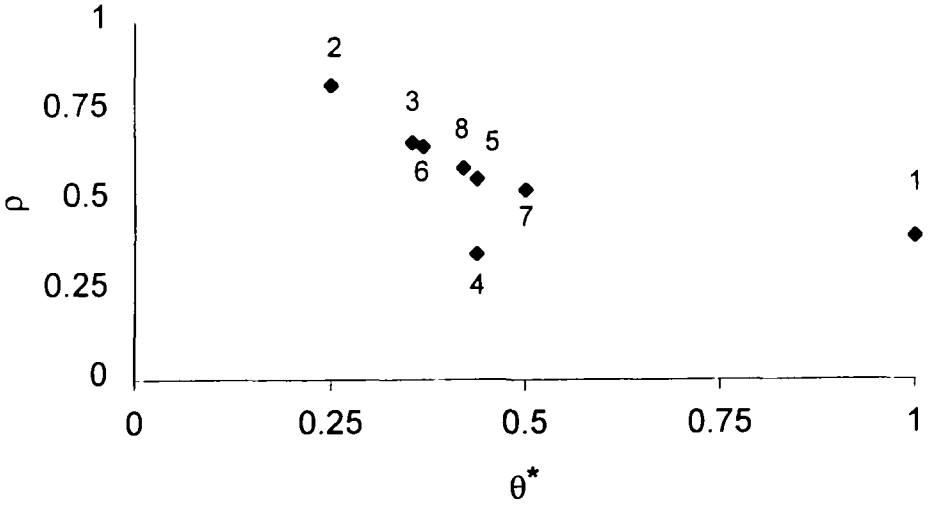

Fig. 7. Relationship between parameter correlation coefficient and the shape index. (A high value for the shape index corresponds to high convexity.)

2 at $I/I_S = 10$, even the light intensity exposed to the upmost bottle is still not within the saturated range and this model will be definitely overparameterized. This is also illustrated in Figure 3, in which the measured and simulated oxygen production rates are plotted for a typical experiment. For the Steele model (model 4), which does include inhibition, high parameter correlation coefficients can be expected if I/I_{opt} is less than one. In that case, it is virtually impossible to estimate I_{opt}.

Model formulations using initial slope α. In the previous evaluation of the *P/I* relationships, the parameters estimated were P_M and I_S. However, the relationships between oxygen production and light intensity can also be formulated in terms of the initial slope (α) and the saturated production (P_M), as has been indicated before. In most limnological and oceanographical literature, the latter formulation is preferred, as P_M and α are the two really independent characteristic parameters describing the curve. I_S is very often considered as a secondary parameter, as it depends on both the initial slope and the saturation level (Zimmerman *et al.*, 1987). For example P_M is considered to be temperature dependent, whereas α is not. Because of the interrelationship between I_S and P_M, I_S will be a function of temperature as well. Henley (1992) states that in this respect I_S very often is no suitable parameter to evaluate the photoacclimation status. For *Ulva rotundata*, he shows that changes in I_S only reflect the changes in P_M. This was also found by Beardall and Morris (1976) for phytoplankton.

Models 1–8 presented in Table II have been reformulated by substitution of $I_S = P_M/\alpha$.

For the Wolderwijd data set, the parameters were estimated once again. As could be expected, the resulting sum of squared residuals did not change, except for some minor differences caused by the precision of the estimation procedure (see Table VI, which presents total sum of squares, averaged parameter coefficients of variation and correlation coefficients). Also, the estimated P_M values did not change and the values for α almost exactly equalled P_M/I_S (not shown). However, with respect to the parameter correlation and the coefficients of variation of the individual parameters, the results differ remarkably. The coefficient of variation for P_M did not differ for the two model formulations. However, for some of the models, the coefficient of variation for α was found to be lower than that for I_S. The difference is most profound for model 2 and only limited for

Table VI. Overall results using initial slope (α) formulation applied to Lake Wolderwijd data

Model	Grand *SSE*	CV P_M (%)	CV α (%)	ρ
1	3.02	8.6	23.4	0.00
2	2.92	16.8	48.1	–0.72
3	2.88	11.2	34.8	–0.47
4	3.38	10.5	21.0	0.45
5	2.69	10.0	29.1	–0.32
6	2.71	11.6	33.8	–0.47
7	2.73	9.5	28.4	–0.25
8	2.84	10.1	30.1	–0.35

models 7 and 1, and virtually absent in model 4. The relative decrease in the coefficient of variation for α is related to the convexity of the *P/I* curve. For increasing convexity of the *P/I* curve, the decrease in the coefficient of variation is less prominent. Zimmerman *et al.* (1987) show that the variance of α can be obtained from:

$$var(\alpha) = h \cdot COV \cdot h^{T} \tag{19}$$

where *COV* is the covariance matrix according to equation (11) and h is the vector given by:

$$\left[\frac{\partial \alpha}{\partial P_M}, \frac{\partial \alpha}{\partial I_S}\right] \tag{20}$$

Substitution of equation (11) leads to:

$$var(\alpha) = \frac{var(P_M) - 2\alpha COV(P_M, I_S) + \alpha^2 var(I_S)}{I_S^2} \tag{21}$$

For high covariance between P_M and I_S, the variance of α will be smaller, as can be seen from equation (21). As for the low-convexity models, the covariance between P_M and I_S is higher; this explains why the relative decrease in the coefficient of variation for these models is more distinguished.

Except for model 4, the parameter correlation is also decreasing using the α formulation. The highest reduction in ρ was found for model 7. In this case, the correlation coefficient decreased by a factor 2. The lowest reduction was found for model 2. For model 1, the resulting correlation coefficient between the parameters is zero by definition as α and P_M are totally independent. Overall, it can be concluded that using the initial slope, instead of I_S, leads to lower parameter correlation, in particular for the highly convex models. However, for these models parameters correlation estimating I_S was not really a problem anyway. Especially for model 2, the low-convexity model parameter, correlation may still be high.

The use of nett oxygen production data. In the previous analysis, the gross oxygen production rates were used to estimate the model parameters. Gross oxygen production rates were calculated by subtracting the oxygen content in dark bottles from the light bottle concentration at the end of the exposure time. Nett oxygen production can be calculated directly from the light bottle oxygen content and the initial oxygen concentration in the bottles. As the error in the initial oxygen concentration is small compared to the concentration in the dark bottles, the overall error in the nett oxygen production is expected to be smaller than that in gross production rates. For all models, the parameters were estimated once again using nett oxygen production rates, applying equation (4). Hence, the oxygen consumption rate, R_{ox}, had to be estimated as an additional parameter. Figure 8

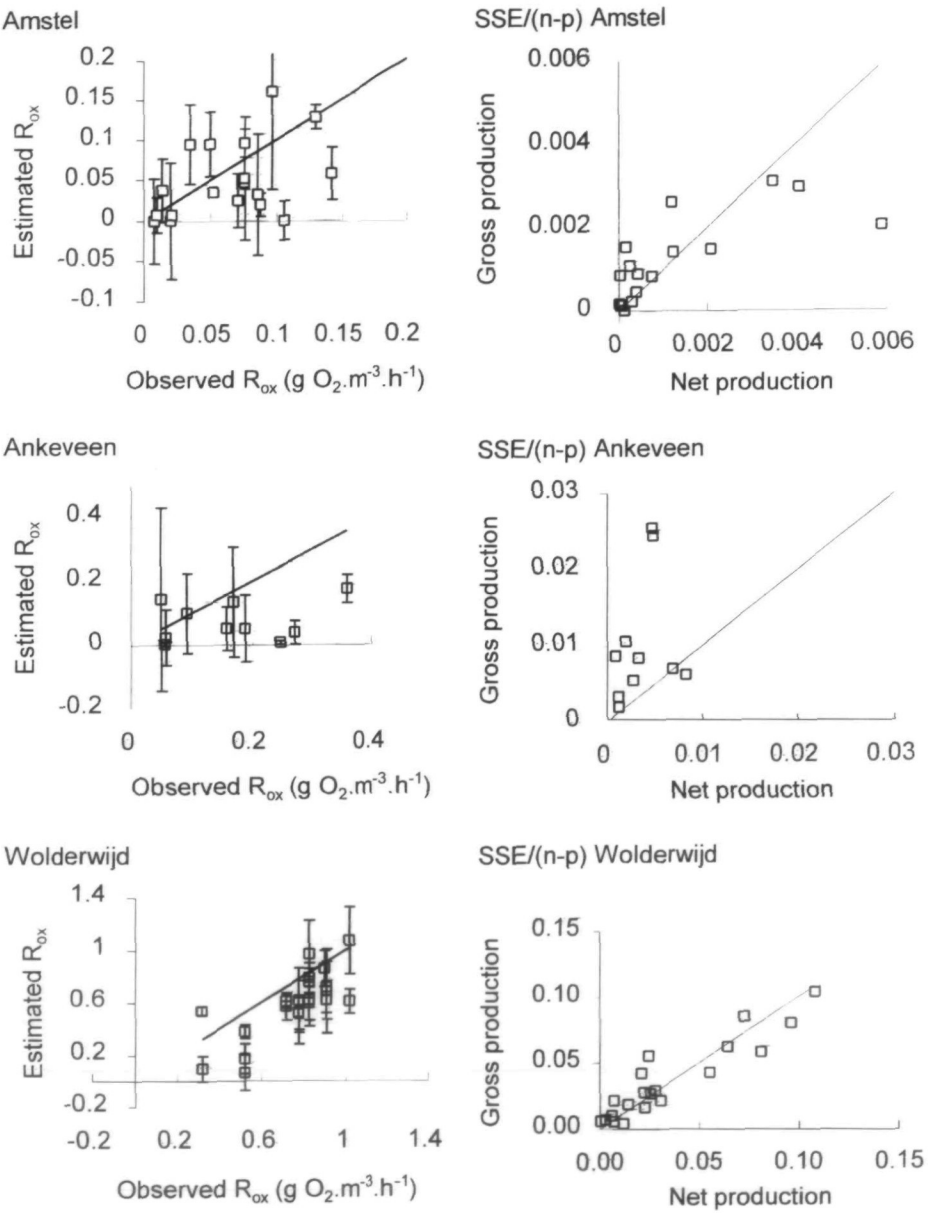

Fig. 8. Comparison of estimated and measured oxygen consumption rates, using nett and gross oxygen production data.

shows the results for model 7 using the initial slope formulation. For the other models, the overall results showed similar tendencies as for model 7. Model 7 was selected as this model appeared to be the least sensitive for parameter correlation between P_M and α.

All experiments produced a lower sum of squared errors, when using nett production data. However, after correction for the degrees of freedom $(n - p)$ for most experiments, no significant difference in goodness of fit was found. For the Wolderwijd data, the ratio of the corrected sum of squared errors is (except for one experiment) always less than three, indicating that there is no significantly better fit for one of the methods. For a difference to be significant at a 90% confidence level, the ratio should be 5.3. For the Amstel and Ankeveen data, there are, respectively, four and two experiments showing an F ratio higher than 5.3. For all three data sets, the lower $SSE/(n - p)$ values using nett production are found in particular for the experiments showing both low production and consumption rates. In these cases, the measurement error in R_{ox} contributes relatively strongly to the sum of squared errors. At high production rates, this contribution is less important. Consequently, considering the goodness of fit, it can be concluded that the use of nett production does not result in a better fit of the model. Only at low productivity can a superior description be expected.

For the Wolderwijd data, in most experiments the measured R_{ox} is higher than the estimated value. The Ankeveen data show a similar tendency. As the oxygen consumption rates for the Amstel data are very low and within the range of experimental error, no clear distinction between measured and estimated R_{ox} can be found here.

The discrepancy between the measured and estimated R_{ox} raises the question whether dark bottle experiments do give a representative value for respiration and can be used to calculate gross oxygen production. As R_{ox} reflects the total community respiration, first of all a distinction between algal and non-algal respiration must be made. Cohen (1990) tried to fractionate phytoplankton and non-phytoplankton respiration by regression of the measured dark respiration against Chl *a* to obtain a *y* intercept, representing the non-algal oxygen consumption. For the Wolderwijd data, this generated an intercept of 0.37 mg O_2 l^{-1} h^{-1} and a slope of 0.0021 mg O_2 μg^{-1} Chl *a* h^{-1} ($R^2 = 0.80$), indicating that a considerable part of the overall oxygen consumption is caused by algal respiration. At a biomass level of 100–300 μg Chl *a* l^{-1} (lower and upper limit of observed range), this results in a contribution of phytoplankton respiration to the total oxygen consumption rate of 40–60%. For the Ankeveen data set, a similar relationship was found, although in this case the scatter was somewhat higher ($R^2 = 0.70$). Probably, much of the scatter is due to variations in the non-phytoplankton respiration, but it is also well known that the algal respiration rate can be highly variable between species. Furthermore, it depends on the physiological condition and nutrient availability (Burris, 1980). The Amstel data did not show a relationship between the algal biomass and oxygen consumption rate.

The difference between the estimated and observed R_{ox} can be explained by dark respiration, taking place both in the light and dark, and photorespiration, which occurs in the light only. Dark respiration reflects mitochondrial respiration and is due to the oxidation of organic compounds, thus producing ATP which is used for cell maintenance and growth. In a review on dark respiration, both Harris and Piccinin (1977) and Burris (1980) show that it is likely that dark respiration is limited in the light as many investigators do find elevated dark

respiration rates in the dark. The results from the Wolderwijd and Ankeveen data, showing higher observed R_{ox} values in the dark, are in agreement with these findings (see Figure 8). As the estimates of the dark respiration rate resulting from the dark bottle experiments are not representative for the light bottle respiration rates, the parameters resulting from gross oxygen data are likely to be biased. They definitely will affect P_M, but might also have an influence on the shape of the *P/I* curve, as it is likely that the influence will not be the same for all bottles.

Also, photorespiration could lead to non-representative estimates of dark respiration. Photorespiration is also a light-dependent process and is considered to be caused by the biosynthesis and oxidation of low-molecular-weight carbohydrates (Burris, 1980). The process is very often demonstrated by the decrease in total respiration after switching off the light. Stone and Ganf (1981) studied photorespiration in four species of freshwater algae after short exposure to saturating light intensities and found the total respiration to decrease exponentially until a stationary level was reached. From their data, a typical time constant for the decline of total respiration is of the order of 10–30 min. Markager *et al.* (1992) reported a similar time constant for an *Oscillatoria*-dominated community. If photorespiration occurs, the respiration obtained from dark bottle experiments will also not be representative and will depend on the exposure time. Assuming a typical time constant of 30 min and dark bottle exposure time of 2–3 h, this will produce an overestimation of the dark respiration, as only after 1.5 h the effect of photorespiration will have disappeared and a stationary respiration level will be reached. It has been demonstrated that photorespiration is influenced by both the preceding light intensity and exposure time, and occurs at intensities above the saturating level. This has been explained by the formation of low-molecular-weight products of photosynthesis, which accumulate at high light intensities and long exposure times. After darkening, the accumulated pool of substrate is exhausted, resulting in an exponential decrease in the total respiration rate. As photorespiration is light dependent, it is likely that the influence will be most prominent in the uppermost bottles. In the lower bottles, the total respiration will resemble the dark bottle respiration. Using dark bottle oxygen concentrations to calculate gross oxygen production will result in an underestimation of gross oxygen production at high light intensities. Hence, the use of gross oxygen production data is likely to lead to biased estimates of P_M and I_S as well.

Discussion

P/I models are merely empirical relationships relating *P* to incident light intensities. For all eight models investigated, the mathematical structure is different. As the models are more or less black box type of models, there is no *a priori* best model. We investigated which mathematical representation of the curve did describe the data best. The results showed that there is no best model with respect to goodness of fit, based on the data we used. Although the number of measured *P* values for each curve is limited to five or six, other studies using light and dark bottles or other incubator experiments with more observations also show that

there is not one general model that fits the data best (Lederman and Tett, 1981; Field and Effler, 1982; Nicklisch, 1992). This is because the experimental error is still too high to discriminate between models even at a greater number of *P/I* measurements. Tschumi *et al.* (1978) report a minimum error related to Winkler oxygen measurements of ~0.024 mg O_2 l^{-1}. Using a one-sided *t*-test at 5% significance and correcting for the small number of samples, they calculate a least significant difference between two means of triplicate measurements of 47 μg l^{-1}. From multiple parallel measurements from the Amstel dataset, an estimate of the standard deviation for the initial oxygen concentration of 0.053 mg l^{-1} was obtained, resulting in a precision of 104 μg l^{-1}. This precision is based on the assumption that the measurement error is only determined by the Winkler method, but the Amstel data showed that the standard deviation for dark and light bottle measurements was 0.098 and 0.193 mg l^{-1}, respectively (at 3 h exposure time). This indicates that much of the variation is due to other factors. Probably, both differences in biomass and in light exposure are responsible for the variability between the experiments. Using triplicate experiments, the least significant (5%) precision for gross and nett oxygen production is ~0.27 and 0.30 mg l^{-1}. For respiration, a best obtainable precision of 0.15 mg l^{-1} was found. Comparing the precision of the measurements with the differences between the models supports the conclusion that it is not possible to discriminate between the models on the basis of goodness of fit.

Although the models cannot be distinguished on the basis of goodness of fit, they do differ in the resulting parameter uncertainty. It has been shown that this is related to the shape of the resulting *P/I* curves. In particular, low-convex models will, due to high parameter correlation, show a tendency for wide elongated confidence regions. The parameters estimated from these models will be less well determined. As the low-convex models are more sensitive to overparameterization, for these models more attention to the experimental design is required. For example, model 2 still results in high parameter correlation at I/I_S ratios up to 10 or more. By proper experimental design, i.e. an adequately selected distribution over the *P/I* curve, overparameterization can of course be prevented. However, for light and dark bottle experiments, this is difficult. Especially in turbid shallow systems, experimental limitations will confine the possibilities.

The use of the initial slope and P_M produces lower correlation coefficients. Hence, this formulation will be less sensitive for overparameterization. However, the reduction is limited to the low-convexity models.

Another point of discussion that should be addressed is the transferability of parameters from one model to another. It has been argued that the estimated parameter values will depend on the model used. Figure 9 compares the values for P_M and α estimated from models 2 and 7, using the Wolderwijd data. As could be foreseen, the low-convex model 2 tends to result in higher values for P_M and α. This will definitely be the case if only one or no data in the light-saturated range are available. Henley (1993) states that models with a low convexity tend to overestimate α, as in general *P/I* data do show high convexity. This is supported by Leverenz *et al.* (1990). They showed that for many green plant cells the convexity

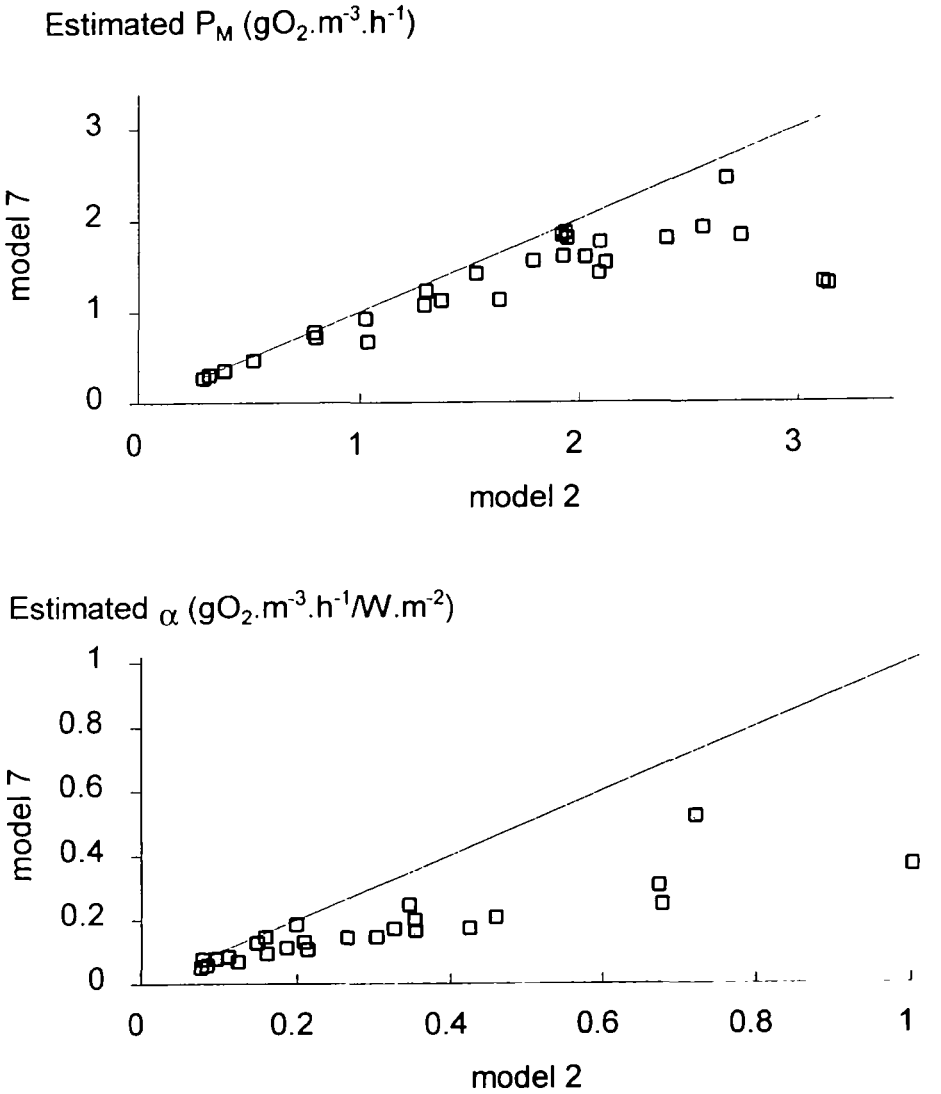

Fig. 9. Comparison of the estimated P_M and α values from Wolderwijd data, using models 2 and 7.

of *P/I* data is high. For many unstressed plants, including algae, the value of $\theta_{0.5}$ [equation (17)] may be between 0.97 and 0.98.

It has thus been shown that although there is no best model with respect to goodness of fit, the selection of an appropriate model is vital with respect to the estimated parameter values and their confidence intervals. In particular, when parameters are estimated in order to study the photoacclimation of algae or the influence of environmental conditions, this should be recognized. This is once again illustrated in Figure 10. This figure presents the relationship between the depth-averaged irradiance and the specific light efficiency (α/Chl *a*). As can be

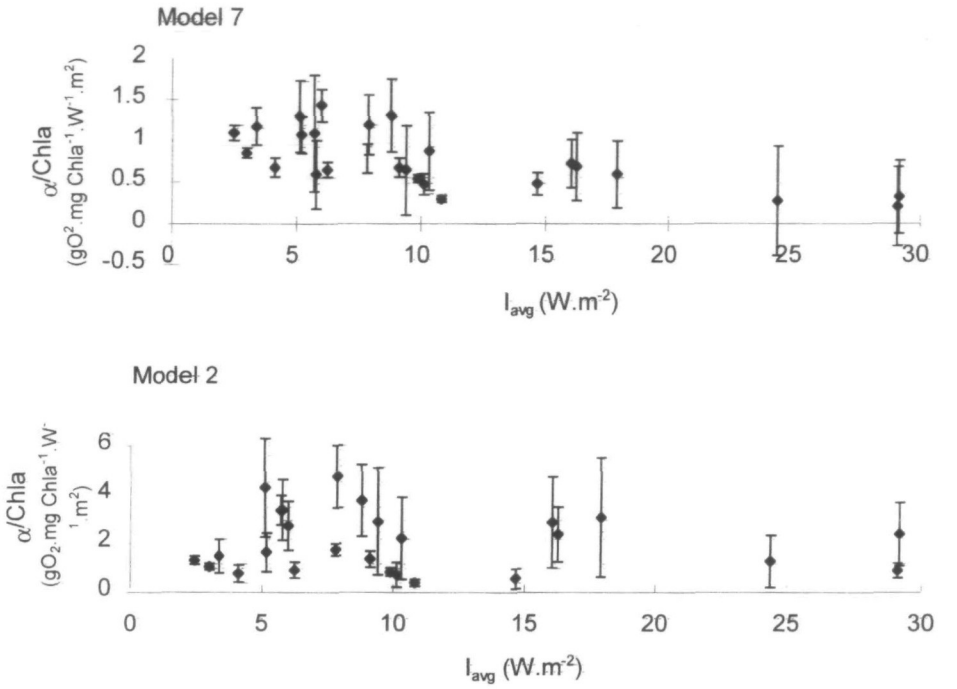

Fig. 10. Relationship between α/Chl *a* and depth-averaged light intensity during the exposure time.

seen, using model 7 a relationship between efficiency and light intensity was found, but using model 2 hardly any dependency can be observed. A decrease in efficiency at elevated irradiance is a well-known phenomenon (Falkowski *et al.*, 1985; Smith *et al.*, 1989). That for model 7 the relationship is also not very distinct could be expected as the data were gathered during two different years, and variations in both the population and the physiological status of the algae are likely. Additionally, it is well known that the efficiency is controlled by the light history as well and correlation with incident irradiance is likely to be poor.

Conclusions

As the experimental error in the oxygen production rates obtained from the light and dark bottle experiments made in this study is too high, no discrimination can be made between the eight models tested. Comparison of the sum of squared errors did not show significant differences (at a 90% confidence level) in goodness of fit (see Table IV and Figure 5). This is in agreement with the results of other authors (Lederman and Tett, 1981; Field and Effler, 1982; Nicklisch, 1992) as also from their comparative studies it is hard to distinguish between different models.

Although all eight models do describe the observed oxygen production equally well, they do show distinct differences with respect to parameter correlation. In

particular, the *P/I* curve with lowest convexity (i.e. model 2) suffers from overparameterization (Figure 6). As the correlation between the parameters depends on the distribution of the observations over the *P/I* curve, experimental design is important in conducting experiments to identify the relationship between intensity and photosynthetic rate. However, for light and dark bottle experiments, this is not easy. Particularly in shallow turbid water, it is hard to meet the requirement of a good distribution of the observations over the curve.

For calculating depth-integrated production, parameter correlation is not really a problem, but for studying parameter dependency on environmental conditions it is, as experiments showing high parameter correlation will not result in unique estimates of the parameters, as there are many combinations of P_M and I_S which describe the observed oxygen production equally well. Hence, if the main objective of light and dark bottle experiments is to estimate P_M and I_S (or α), preferably one of the high-convex curves (model 4, 5, 7 or 8) should be selected. This statement is further justified by the fact that many *P/I* data show a high convexity and consequently the use of a low-convex curve is likely to result in biased estimates of the parameters.

The use of α, the initial slope, instead of I_S results in lower correlation coefficients. This is particularly the case for the highly convex models. For the models showing low convexity, the reduction in correlation is limited.

It has been shown that the use of dark bottles or direct estimation of R_{ox} does not make any difference with respect to goodness of fit. Again, experimental errors are too high to discriminate between the two methods. However, observed respiration rates from dark bottle experiments tend to be higher than those estimated from light bottle data only (see Figure 8). Hence, it can be questioned whether observed R_{ox} values are representative for the oxygen consumption in the light bottles.

References

Aalderink,R.H., van Alphen,J.C.A., Mankor,J. and de Smit,D. (1994) Toepassing van de modellen DYNHYD and EUTROWASP op de boezem van Amstelland-west. *H_2O*, **27**, 534–541.

Baly,E.C.C. (1935) The kinetics of photosynthesis. *Proc. R. Soc. London Ser. B*, **117**, 218–239.

Bard,Y. (1974) *Non Linear Parameter Estimation*. Academic Press, New York, 341 pp.

Beardall,J. and Morris,I. (1976) The concept of light intensity adaptation in marine phytoplankton: some experiments with *Phaeodactylum tricornutum*. *Mar. Biol.*, **37**, 377–387.

Blackman,F.F. (1905) Optima and limiting factors. *Ann. Bot.*, **19**, 281–295.

Burris,J.E. (1980) Respiration and photo-respiration in marine algae. In Falkowski,P.G. (ed.), *Primary Productivity in the Sea*. Plenum Press, New York.

Cohen,R.R.H. (1990) Biochemical oxygen demand and algae: Fractionation of phytoplankton and non-phytoplankton respiration in a large river. *Water Resour. Res.*, **26**, 671–678.

Côté,B. and Platt,T. (1984) Utility of the light-saturation curve as an operational model for quantifying the effects of environmental conditions on phytoplankton photosynthesis. *Mar. Ecol. Prog. Ser.*, **18**, 57–66.

Denman,K.L. and Marra,J. (1986) Modelling the time dependent photo-adaptation of phytoplankton to fluctuating light. In Nihoul,J.C.L. (ed.), *Marine Interface Ecohydrodynamics*. Elsevier, Amsterdam, pp. 341–349.

Draper,N.R. and Smith,H. (1981) *Applied Regression Analysis*. John Wiley & Sons, New York.

Eilers,P.H.C. and Peeters,J.C.H. (1988) A model for the relationship between light intensity and the rate of photosynthesis in phytoplankton. *Ecol. Model.*, **42**, 199–215.

Eilers,P.H.C. and Peeters,J.C.H. (1993) Dynamic behaviour of a model for photosynthesis and photoinhibition. *Ecol. Model.*, **69**, 113–133.

Falkowski,P.G. (1981) Light-shade adaptation and assimilation numbers. *J. Plankton Res.*, **3**, 203–216.
Falkowski,P.G., Dubinsky,Z. and Santostefano,G. (1985) Light-enhanced dark respiration in phytoplankton. *Verh. Int. Ver. Limnol.*, **22**, 2830–2833.
Fasham,M.J.R. and Platt,T. (1983) Photosynthetic response of phytoplankton to light: a physiological model. *Proc. R. Soc. London Ser. B*, **219**, 355–370.
Field,S.D. and Effler,S.W. (1982) Photosynthesis-light mathematical formulations. *J. Environ. Eng. Div. ASCE*, **108**, 199–203.
Field,S.D. and Effler,S.W. (1984) Light-productivity model for Onondage lake, N.Y. *J. Environ. Eng. Div. ASCE*, **109**, 830–844.
Gallegos,C.L. and Platt,T. (1981) Photosynthesis measurements on natural populations of phytoplankton: numerical analysis. *Can. Bull. Fish. Aquat. Sci.*, **210**, 103–112.
Harris,G.P. (1984) Phytoplankton productivity and growth measurements: past, present and future. *J. Plankton Res.*, **6**, 219–235.
Harris,G.P. and Piccinin,B.B. (1977) Photosynthesis by natural phytoplankton populations. *Arch. Hydrobiol.*, **80**, 405–457.
Henley,J.H. (1992) Growth and photosynthesis of *Ulva rotundata* (Chlorophyta) as a function of temperature and square wave irradiance in indoor cultures. *J. Phycol.*, **28**, 625–634.
Henley,J.H. (1993) Measurements and interpretation of photosynthetic light-response curves in algae in the context of photo-inhibition and diel changes. *J. Phycol.*, **29**, 729–739.
Jassby,A.D. and Platt,T. (1976) Mathematical formulation of the relationship between photosynthesis and light for phytoplankton. *Limnol. Oceanogr.*, **21**, 540–547.
Kirk,J.T.O. (1977) Attenuation of light in natural waters. *Aust. J. Mar. Freshwater Res.*, **28**, 497–508.
Lederman,T.C. and Tett,P. (1981) Problems in modelling the photosynthesis-light relationship for phytoplankton. *Bot. Mar.*, **XXIV**, 125–134.
Leverenz,J.W., Falk,S., Pilström,C.M. and Samuelsson,G. (1990) The effect of photo-inhibition on the photosynthesis light-response curve of green plant cells (*Chlamydomonas reinhardtii*). *Planta*, **182**, 161–168.
Lewis,M.R., Cullen,J.J. and Platt,T. (1984) Relationships between vertical mixing and photoadaptation: similarity criteria. *Mar. Ecol. Prog. Ser.*, **15**, 141–149.
Markager,S., Jespersen,A.M., Madsen,T.V., Berdalet,E. and Weisburd,R. (1992) Diel changes in dark respiration in a plankton community. *Hydrobiologia*, **238**, 119–130.
Megard,R.O., Tonkyn,D.W. and Senft,W.H. (1984) Kinetics of oxygenic photosynthesis in planktonic algae. *J. Plankton Res.*, **6**, 325–337.
Neale,P.J. and Marra,J. (1985) Short-term variation of P_{max} under natural irradiance conditions: a model and its implications. *Mar. Ecol. Prog. Ser.*, **26**, 113–124.
Nicklisch,A. (1992) The interaction of irradiance and temperature on the growth rate of *Limnothrix redekei* and its mathematical description. *Algol. Stud.*, **63**, 1–18.
Pahl-Wostl,D and Imboden,D.M. (1990) DYPHORA — a dynamic model for the rate of photosynthesis of algae. *J. Plankton Res.*, **12**, 1207–1221.
Peterson,D.H., Perry,M.J., Bencala,K.E. and Talbot,M.C. (1987) Phytoplankton productivity in relation to light intensity: a simple equation. *Estuarine Coastal Shelf Sci.*, **24**, 813–832.
Platt,T. and Gallegos,C.L. (1980) Modelling primary production. In Falkowski,P.G. (ed.), *Primary Production in the Sea*. Plenum Press, New York, pp. 339–362.
Platt,T., Gallegos,C.L. and Harrison,W.G. (1980) Photo-inhibition of photosynthesis in natural assemblages of marine phytoplankton. *J. Mar. Res.*, **38**, 687–701.
Press,W.H., Flannery,B.P., Teulkolsky,S.A. and Vetterling,W.T. (1989) *Numerical Recipes in Pascal. The Art of Scientific Computing*. Cambridge University Press, Cambridge.
Prioul,J.L. and Chartier,P. (1977) Partitioning of transfer and carboxylation components of intracellular resistance to photosynthesis CO_2 fixation: A critical analysis of the methods used. *Ann. Bot.*, **41**, 789–900.
Richter,O. and Söndgerath,D. (1990) *Parameter Estimation in Ecology. The Link Between Data and Models*. VCH Publishers, New York.
Roijackers,R.M.M. and Verstraelen,P.J.T. (1988) Ecological investigations in three shallow lakes of different trophic level in the Netherlands. *Verh. Int. Ver. Limnol.*, **23**, 489–495.
Sakamoto,M. *et al.* (1984) Joint field experiments for comparisons of measuring methods of photosynthetic production. *J. Plankton Res.*, **6**, 365–383.
Smith,E.L. (1936) Photosynthesis in relation to light and carbon dioxide. *Proc. Natl Acad. Sci. USA*, **22**, 504–511.
Smith,R.C., Prézelin,B.B., Bidigare,R.R. and Baker,K.S. (1989) Bio-optical modelling of photosynthetic production in coastal water. *Limnol. Oceanogr.*, **34**, 1524–1544.
Steele,J.G. (1962) Environmental control of photosynthesis in the sea. *Limnol. Oceanogr.*, **7**, 137–150.

Stone,S. and Ganf,G. (1981) The influence of previous light history on the respiration of four species of freshwater phytoplankton. *Arch. Hydrobiol.*, **91**, 435–462.
Talling,J.F. (1957) Photosynthesis characteristics of some freshwater plankton diatoms in relation to underwater radiation. *New Phytol.*, **56**, 29–50.
Talling,J.F. (1984) Past and contemporary trends and attitudes in work on primary productivity. *J. Plankton Res.*, **6**, 203–217.
Tank,L.T. and Musson,J.C. (1993) An inexpensive chamber apparatus for multiple measurement of dissolved oxygen uptake or release. *J. North Am. Benthol. Soc.*, **12**, 406–409.
Tschumi,P.A., Zbären,D. and Zbären,J. (1978) An improved oxygen method for measuring primary production in lakes. *Verh. Int. Ver. Limnol.*, **20**, 43–48.
van Duin,E.H.S. and Lijklema,L. (1989) Modelling photosynthesis and oxygen in a shallow hypertrophic lake. *Ecol. Model.*, **45**, 243–260.
van Duin,E.H.S., Aalderink,R.H. and Lijklema,L. (1995) Light adaptation of *Oscillatoria agardhii* at different time scales. *Water Sci. Techn.*, **32**, 35–48.
van Straten,G. and Herodek,S. (1982) Estimation of algal growth parameters from vertical primary production profiles. *Ecol. Model.*, **15**, 287–311.
Vollenweider,R.A. (1974) *A Manual on Methods for Measuring Primary Production in Aquatic Environment. IBP Handbook No. 12.* Blackwell Scientific, Oxford.
Web,W.L.M., Newton,M. and Starr,D. (1974) Carbon dioxide exchange of *Alnus rubra*: a mathematical model. *Oecologia (Berlin)*, **17**, 281–291.
Zimmerman,R.C., Beeler Soohoo,J., Kremer,J.N. and D'Argenio,D.Z. (1987) Evaluation of variance approximation techniques for non-linear photosynthesis-irradiance models. *Mar. Biol.*, **25**, 209–215.

Received on March 31, 1997; accepted on July 11, 1997